

ORGANIC CHEMISTRY

Intermolecular dialkylation of alkenes with two distinct C(sp³)—H bonds enabled by synergistic photoredox catalysis and iron catalysis

Xuan-Hui Ouyang^{1*}, Yang Li^{1*}, Ren-Jie Song^{1†}, Ming Hu¹, Shenglian Luo¹, Jin-Heng Li^{1,2,3†}

The functionalization of unactivated C(sp³)—H bonds represents one of the most powerful and most atom-economical tools for the formation of new carbon-based chemical bonds in synthesis. Although cross-dehydrogenative coupling reactions of two distinct C—H bonds for the formation of carbon-carbon bonds have been well investigated, controlled functionalizations of two or more different C(sp³)—H bonds across a functional group or a molecule (e.g., an alkene or alkyne) in a single reaction remain challenging. Here, we present a three-component dialkylation of alkenes with common alkanes and 1,3-dicarbonyl compounds via synergistic photoredox catalysis and iron catalysis for the synthesis of two functionalized 1,3-dicarbonyl compounds. Mechanistic studies suggest that the photoredox catalysis serves as a promotion system to allow the dialkylation to proceed under mild conditions by reducing the oxidation and reduction potentials of the iron intermediates and the reaction partners.

INTRODUCTION

The development of a mild, economical, and practical catalytic process that can selectively and rapidly increase molecular complexity starting from readily available materials, especially petroleum-based feedstocks (e.g., alkenes, alkanes, and arenes), is a critical objective in both the academic and industrial communities. In this field, the functionalization of a molecule through transformations of an alkene and/or C—H bonds is a particularly fascinating but challenging goal, which has therefore attracted substantial attention from chemical researchers. Typical technologies include alkene dicarbofunctionalizations that enable the concomitant incorporation of two vicinal carbon-based functional groups to lengthen carbon chains and increase structural complexity (1–4). However, the vast majority of alkene dicarbofunctionalization approaches focus on the merger of the classical cross-couplings (1–18), which suffer from requiring expensive nucleophilic and electrophilic functional reagents, such as organometallic species and organohalides, for inserting the C=C bonds in the presence of noble transition metals and/or ligands. Moreover, examples that allow the addition of alkyl groups across alkenes to achieve dicarbofunctionalization are rare; this is partly because competitive side reactions, such as the Heck-type β-hydride elimination, homocoupling, isomerization, and/or protodemetalation, are common in these types of reactions (5–18).

Alternatively, alkene dicarbofunctionalizations via the oxidative radical functionalization of one or two C—H bonds has attracted increasing interest in the past few years because it features excellent selectivity, high atom economy, and cost efficiency by avoiding the use of expensive functional reagents and noble metals (19–21). However, the number of available methods is much lower, and methods are limited to two modes, alkylation (22–26) and acylation (27, 28), which are accomplished via an intramolecular inherent aryl C(sp²)—H cyclization process to prepare cyclic compounds at high reaction temperatures. Furthermore, to the best of our knowledge, examples of

using two distinct C(sp³)—H bonds in the intermolecular dialkylation of alkenes has not been reported, as controlled functionalizations of two or more distinct C(sp³)—H bonds across a functional group or a molecule (e.g., an alkene or alkyne) in a single reaction is challenging.

Merging visible light photoredox catalysis with transition metal catalysis has become a conceptually powerful strategy for the formation of chemical bonds owing to its extraordinary catalytic activity and mild conditions (29–32), and this method has also been applied to the functionalization of C(sp³)—H bonds (29–37). In these radical processes, selectivity and reactivity could be manipulated mainly through tuning the oxidation and reduction potentials of the reaction partners and catalysts (29–32). We envisioned that using photoredox and transition metal catalysts cooperatively might allow the controlled and simultaneous transformation of an alkene with two or more C(sp³)—H bonds under mild conditions by regulating the oxidation and reduction potentials. Here, we report a new radical-mediated intermolecular 1,2-dialkylation of terminal alkenes with two distinct C(sp³)—H bonds enabled by synergistic photoredox catalysis and iron catalysis (Fig. 1). The activation of two distinct C(sp³)—H bonds for insertion across C=C bonds is disclosed for the first time, and in this reaction, a C(sp³)—H bond of a cycloalkane, linear alkane, or ether serves as an sp³-hybridized carbon-centered radical precursor to initiate this reaction, and the other C(sp³)—H bond, α to a 1,3-dicarbonyl fragment, terminates this reaction. Notably, such multifunctional 1,3-dicarbonyl compounds are among the most common and versatile building blocks in synthesis, and they are privileged structural units in natural products, bioactive molecules, and materials.

RESULTS

Optimization of the reaction conditions

Initial experiments were performed using three reaction partners, namely, 1-methoxy-4-vinylbenzene (**1a**), cyclohexane (**2a**), and ethyl 3-oxo-3-phenylpropanoate (**3a**), by merging photoredox catalysis and iron catalysis (Table 1). The use of Fe(OTf)₂ as the metal catalyst and Eosin Y as the visible light catalyst in the presence of 2 equiv of di-*tert*-butyl peroxide (DTBP) and a 5-W blue light-emitting diode (LED) light at 30°C successfully allowed the 1,2-dialkylation of alkene **1a** with **2a** and **3a**, giving the desired product **4aaa** in 82% yield (entry 1).

¹Key Laboratory of Jiangxi Province for Persistent Pollutants Control and Resources Recycle, Nanchang Hangkong University, Nanchang 330063, China. ²Key Laboratory of Chemical Biology and Traditional Chinese Medicine Research (Hunan Normal University), Ministry of Education, Changsha, Hunan 410081, China. ³State Key Laboratory of Applied Organic Chemistry, Lanzhou University, Lanzhou 730000, China. *These authors contributed equally to this work.

†Corresponding author. Email: srj0731@hnu.edu.cn (R.-J.S.); jhli@hnu.edu.cn (J.-H.L.)

However, in the absence of $\text{Fe}(\text{OTf})_2$, only trace gas chromatography (GC) yield of **4aaa** was observed at either 30° or 120°C (entry 2). We found that a lower [10 mole percent (mol %)] or a higher (30 mol %) loading of $\text{Fe}(\text{OTf})_2$ had a negative effect (entries 3 and 4). Other Fe catalysts, including FeCl_2 , $\text{Fe}(\text{acac})_2$, $\text{Fe}(\text{OTf})_3$, and FeCl_3 , were examined (entries 1 and 5 to 7), and each of them was less efficient than $\text{Fe}(\text{OTf})_2$, and the Fe(II) catalysts were more active than the Fe(III) catalysts. Both Eosin Y (entry 8) and DTBP (entry 9) are necessary for the dialkylation to proceed below 100°C (entries 2 to 7), as in the absence

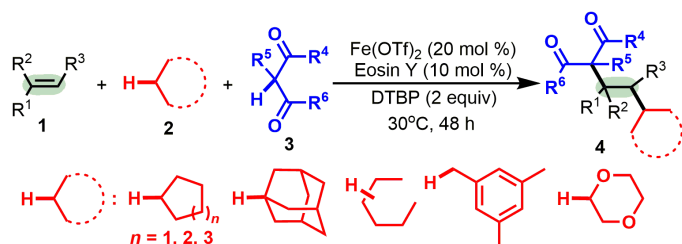


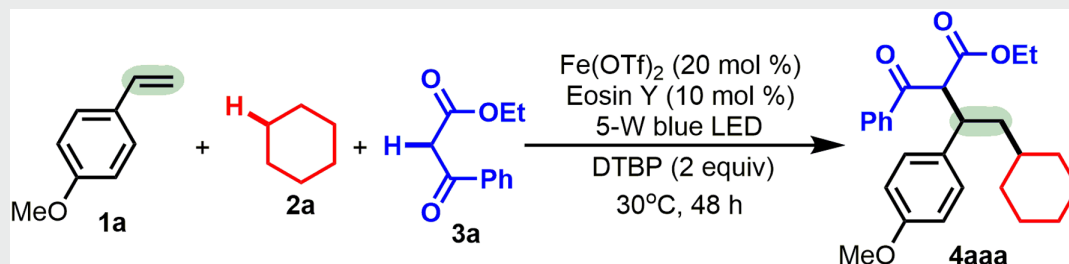
Fig. 1. 1,2-Dialkylation of alkenes with two distinct $\text{C}(\text{sp}^3)\text{—H}$ bonds. Synergistic photoredox catalysis and iron catalysis for the intermolecular dialkylation of alkenes with alkanes and 1,3-dicarbonyl compounds to synthesize two functionalized 1,3-dicarbonyl compounds.

of either, the reaction did not proceed. It is noteworthy that without Eosin Y, the reaction can proceed when the reaction temperature is increased to 110°C (entry 9; 36% yield at 110°C and 80% yield at 120°C), but without DTBP, the reaction does not occur even at 120°C (entry 12). Furthermore, the reaction did not proceed in the dark at 30°C but did generate **4aaa** in 78% yield (entry 15). These results suggest that the photoredox catalyst promotes the reaction, probably by reducing the oxidation and reduction potentials of the iron intermediates. However, other visible light metal catalysts [e.g., $\text{Ru}(\text{bpy})_3\text{Cl}_2$ or $\text{Ir}(\text{ppy})_3$] and peroxides [e.g., *tert*-Butyl hydroperoxide (TBHP) or *tert*-Butyl peroxybenzoate (TBPB)] all proved to be less reactive (entries 10 and 11 and 13 and 14). The reaction proceeded smoothly on scales up to 1 mmol of **1a** (80% yield; entry 16).

Substrate scope with respect to alkenes

With the optimal reaction conditions in hand, we then investigated the generality of this three-component dialkylation protocol with respect to alkenes (Table 2), alkanes, and 1,3-dicarbonyl compounds (Table 3). Under the optimal conditions, this protocol proved amenable to a wide range of terminal alkenes, including arylalkenes **1b** to **1l**, 1,1-disubstituted alkene **1m**, alkylalkene **1n**, and methyl acrylate **1o** but unsuitable for internal alkene **1r** (Table 2). For arylalkenes **1b** to **1l**,

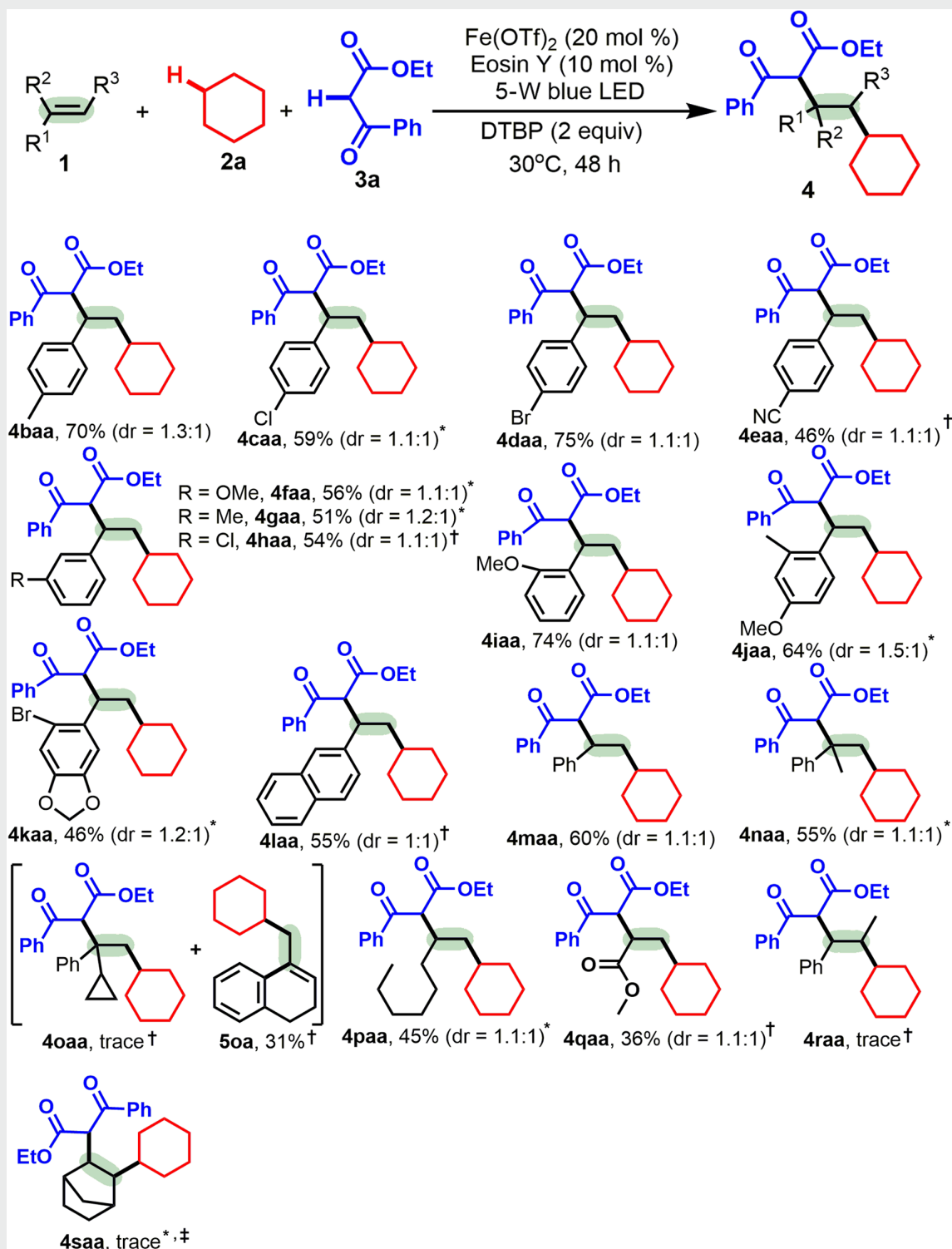
Table 1. Optimization of reaction conditions. Experiments were performed with **1a** (0.2 mmol), **2a** (2 ml), **3a** (2 equiv), $\text{Fe}(\text{OTf})_2$ (20 mol %), Eosin Y (10 mol %), DTBP (2 equiv), 5-W blue LED, argon, 30°C, and 48 hours. The dr value is 1.1:1, as determined by ^1H nuclear magnetic resonance (NMR) analysis of the crude product.



Entry	Variation from the optimal conditions	Isolated yield (%)
1	None	82
2	Without $\text{Fe}(\text{OTf})_2$	Trace*
3	$\text{Fe}(\text{OTf})_2$ (10 mol %) at 60°C	40
4	$\text{Fe}(\text{OTf})_2$ (30 mol %)	53
5	FeCl_2 instead of $\text{Fe}(\text{OTf})_2$	71
6	$\text{Fe}(\text{acac})_2$ instead of $\text{Fe}(\text{OTf})_2$	62
7	$\text{Fe}(\text{OTf})_3$ instead of $\text{Fe}(\text{OTf})_2$	8
8	FeCl_3 instead of $\text{Fe}(\text{OTf})_2$	21
9	Without Eosin Y	Trace ^{††} /36% [§] /80%
10	$\text{Ru}(\text{bpy})_3\text{Cl}_2$ instead of Eosin Y	<5
11	$\text{Ir}(\text{ppy})_3$ instead of Eosin Y	<5/51% [¶]
12	Without DTBP	Trace*
13	TBHP instead of DTBP	22
14	TBPB instead of DTBP	57
15	Without visible light (in the dark)	Trace/31% [‡] /78%
16#	None	80

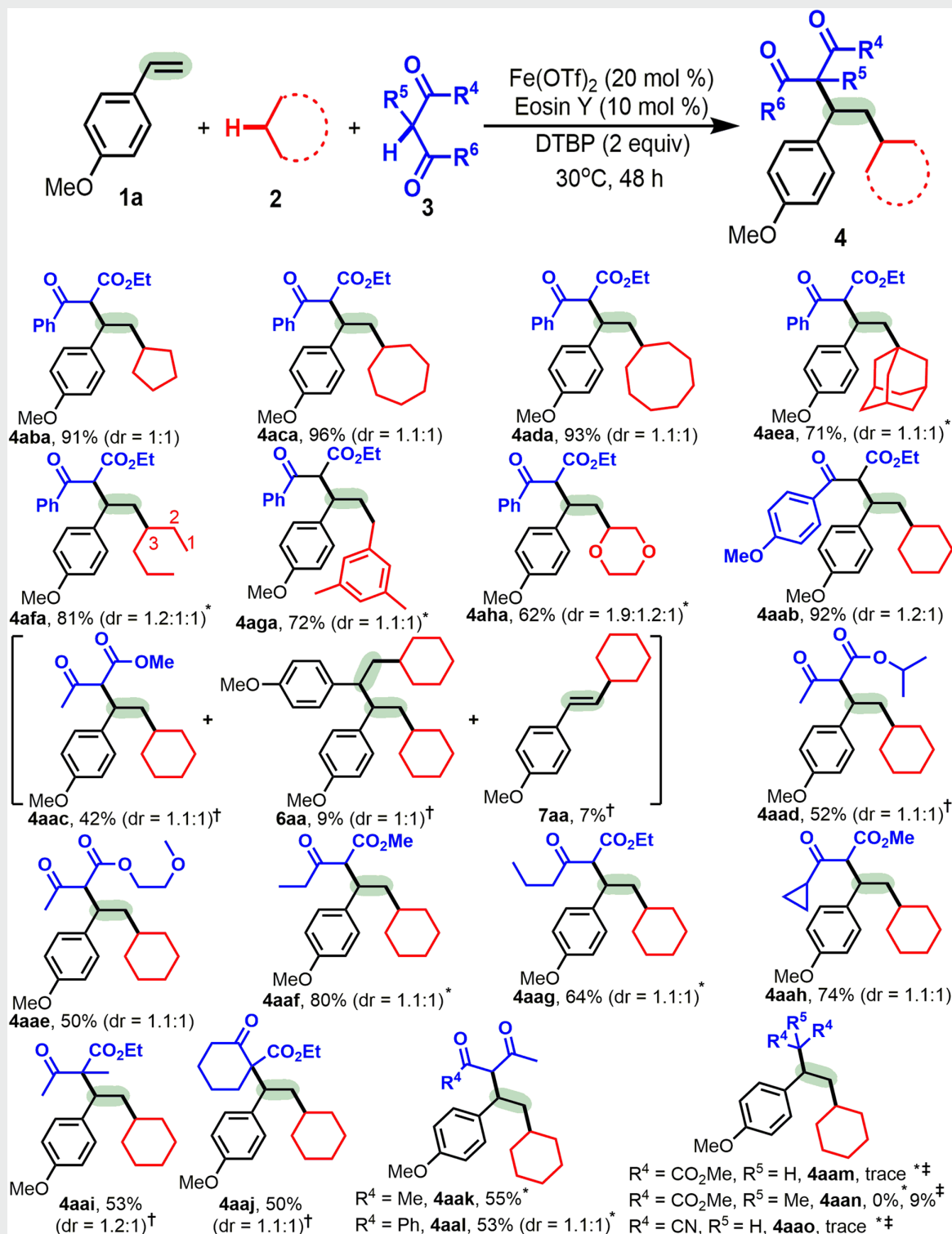
*At 30° or 120°C. [†]At 30° or 100°C. [‡]At 60°C. [§]At 110°C. ^{||}At 120°C. [¶]At 80°C. #**1a** (1 mmol).

Table 2. Variation of the alkene (1). Experiments were performed with **1** (0.2 mmol), **2a** (2 ml), **3a** (2 equiv), Fe(OTf)₂ (20 mol %), Eosin Y (10 mol %), DTBP (2 equiv), 5-W blue LED, argon, 30°C, and 48 hours. The dr value is given in the Supplementary Materials and was determined by ¹H NMR or GC–mass spectrometry (MS) analysis of the crude product.



*At 80°C. [†]At 100°C. [‡]At 130°C without the photocatalyst.

Table 3. Variation of the alkane (2) and 1,3-dicarbonyl compounds (3). Experiments were performed with **1a** (0.2 mmol), **2** (2 ml), **3** (2 equiv), Fe(OTf)₂ (20 mol %), Eosin Y (10 mol %), DTBP (2 equiv), 5-W blue LED, argon, 30°C, and 48 hours. The dr value is given in the Supplementary Materials and was determined by ¹H NMR or GC-MS analysis of the crude product.



several substituents, including Me, Cl, Br, CN, and MeO, on the aryl ring were well tolerated (**4baa** to **4jaa**), and their electronic and steric properties influenced the yields. While alkene **1b** with an electron-donating 4-Me group gave 70% yield of **4baa**, alkene **1e** with an electron-withdrawing 4-CN group afforded 46% yield of **4eaa**. Unexpectedly, *o*-MeO-substituted arylalkene **1i** is more reactive (**4iaa**) than *m*-MeO-substituted alkene **1f** (**4faa**), probably due to the electronic effect more so than the steric effects. Notably, halogen groups, including Cl and Br, are compatible with the optimal conditions and thus provide easy handles for further synthetic elaboration of the halogenated positions (**4caa** to **4daa** and **4kaa**). Using polysubstituted arylalkenes **1j** and **1k** provided **4jaa** to **4kaa**. Both 2-vinylnaphthalene **1l** and styrene **1m** are suitable substrates for constructing **4laa** to **4maa**. Prop-1-en-2-ylbenzene **1n**, a 1,1-disubstituted alkene, was smoothly transformed into **4naa**. However, (1-cyclopropylvinyl)benzene **1o** did not afford **4oaa** and instead generated 4-(cyclohexylmethyl)-1,2-dihydronaphthalene (**5oa**) via ring opening, which supports a radical process (24). Notably, alkylalkene **1p** and electron-poor methyl acrylate **1q** successfully delivered **4paa** to **4qaa**, albeit in reduced yields. Unfortunately, attempts at the 1,2-dialkylation of internal alkene **1r** failed to provide **4raa**.

Substrate scope with respect to alkanes and 1,3-dicarbonyl compounds

As shown in Table 3, a broad scope was also found for the alkane **2** and 1,3-dicarbonyl **3** reaction partners. A number of cycloalkanes, including cyclopentane **2b**, cycloheptane **2c**, cyclooctane **2d**, and bulky adamantane **2e**, underwent 1,2-dialkylation with alkene **1a** and 1,3-dicarbonyl **3a** in good to excellent yields (**4aba** to **4aea**). Using *n*-hexane **2f**, a linear alkane, delivered **4afa** in 81% yield, albeit as a mixture of regioisomers. Notably, the benzyl C(sp³)—H bond of **2g** and the C(sp³)—H bond adjacent to an oxygen atom in **2h** could react to afford corresponding products **4aga** and **4aha**.

The optimized conditions also proved to be tolerant of a wide array of 1,3-keto esters **3b** to **3j** and 1,3-diketones **3k** to **3l** (**4aab** to **4aal**). Ethyl 3-(4-methoxyphenyl)-3-oxopropanoate (**3b**) was highly reactive and afforded 92% yield of **4aab**. However, the reactivity of 3-oxobutanoates **3c** to **3e** was lower, and the products were generated in moderate yields (**4aac** to **4aae**). Notably, two by-products, **6aa** and **7aa**, were observed in the reaction of **3c**. Using 3-oxopentanoate **1f**, 3-oxohexanoate **1g**, or 3-cyclopropyl-3-oxopropanoate **1h** successfully delivered **4aaf** to **4aah** in 64 to 80% yields. Both 2-methyl-3-oxobutanoate **3i** and 2-oxocyclohexane-1-carboxylate **3j** provided challenging quaternary carbon centers, making this an attractive method for synthesis (**4aai** to **4aaj**). 1,3-Diketones **3k** and **3l** were also suitable substrates and provided **4aak** to **4aal**. Unfortunately, diethyl malonate **3m** had no reactivity for accessing **4aam**.

DISCUSSION

Control experiments and mechanistic studies

Control experiments (Table 1 and fig. S2) and the reaction progress with the light on or off over time (fig. S3) show that this alkene 1,2-dialkylation protocol is achieved through cooperative photoredox and iron catalysis (38). Consequently, the mechanisms of this alkene dialkylation reaction were proposed on the basis of the current results and the reported processes (Fig. 3). To further verify it, the loadings of Eosin Y were examined (Fig. 2A). The results demonstrated that the yield of **4aaa** decreased with reducing the Eosin Y

loadings. While in the absence of Eosin Y the dialkylation protocol cannot occur at 30°, 60°, or 100°C under blue light (entry 9; Table 1), using 10 mol % Eosin Y at 60°C led to 31% yield of **4aaa** in the dark (entry 15; Table 1). According to these results and the half-life period data of DTBP (39, 40), the Eosin Y and iron cooperating catalysis might activate DTBP to make DTBP decomposition at lower temperature. Moreover, the cyclic voltammogram experiments indicated that the photocatalyst could modulate the redox potential of the Fe(OTf)₂ catalyst (figs. S4 to S6). It was noted that in the presence of TEMPO, a radical inhibitor, the reaction of alkene **1a** with cyclohexane **2a** and dicarbonyl compound **3a** was completely inhibited, and another product (**10**) from the reaction of cyclohexane **2a** with TEMPO was observed (Fig. 2A). The results suggest that the radical process first generates cyclohexyl sp³-hybridized carbon-centered radical **A** (Fig. 3), which was also supported by the formation of **5oa** (Table 2). In the absence of dicarbonyl compounds **3**, both the Heck-type β-H elimination product **6aa** and the two radicals homocoupling product **7aa** were obtained (Fig. 2C): With enhancing temperatures, yield of **6aa** increased slowly, but yield of **7aa** increased sharply. However, the reaction could not take place without Eosin Y at 30° or 100°C (entry 9 in Table 1 and Fig. 2C). The results support the formation of the 2-cyclohexyl-1-(4-methoxyphenyl)ethyl radical **B** and carbocation **C**. Moreover, the higher temperatures are conducive to the radical **B** forming, and the conversion of the radical **B** into the carbocation **C** is far slower than the radicals homocoupling. In contrast to the results in Table 1, addition of dicarbonyl nucleophiles **3** obviously promotes the generation of the carbocation **C**.

To further understand the mechanism, the cyclic voltammetry experiments of the catalytic system and substrates were conducted to study the redox potential (figs. S4 to S6). Two oxidation peaks of Fe(OTf)₂ were observed at −1.560 V_{SCE} and −0.790 V_{SCE} in CH₃CN, while two reduction peaks appeared on the reverse scan at −0.203 V_{SCE} and −1.000 V_{SCE} (fig. S4). The first oxidation peak of Fe(OTf)₂ was quasi-reversible, and only one electron was transferred in the oxidation process. Ethyl 3-oxo-3-phenylpropanoate (**3a**) (three oxidation peaks) exhibited a higher oxidation potential than cyclohexane (**2a**), implying that **2a** was likely to first undergo oxidative C—H cleavage. As shown in fig. S5, the cyclic voltammogram curve from a mixture of Fe(OTf)₂ and Eosin Y featured an onset oxidation potential of −0.255 V_{SCE} and an oxidation peak at 0.871 V_{SCE} for the oxidation of Fe(II) to Fe(III) with the aid of Eosin Y*, while it featured a reduction peak at −0.416 V_{SCE} and a notable reduction peak at −1.725 V_{SCE}, which makes the Fe(III) reduction very easy. A mixture of multiple component experiments outlined in fig. S6 indicated that both the mixed **1a/2a/3a**/Eosin Y and **1a/2a/3a**/Eosin Y/Fe(OTf)₂/DTBP have one oxidation peak at about 0.763 V_{SCE}, whereas the mixed **1a/2a/3a**/Eosin Y/DTBP has two higher oxidation peaks (0.436 V_{SCE} and 0.742 V_{SCE}). However, the mixed **1a/2a/3a**/Fe(OTf)₂/Eosin Y shows a rather low oxidation peak at 0.845 V_{SCE}, presumably signifying a one-electron reduction event of Fe(OTf)₂ to form the Eosin Y* radical anion. Notably, the Stern-Volmer fluorescence quench experiments were investigated (fig. S7). The emission intensity of Eosin Y is obviously diminished, which is affected by the concentration of Fe(OTf)₂, and is slightly influenced when using DTBP or cyclohexane (**2a**), suggesting that Fe(OTf)₂ provides the electron for the reductive quenching of the Eosin Y* excited state.

Consequently, DTBP may be readily split into the *tert*-butoxyl radical (38) with the aid of photoredox (29–37) and iron (19–28) synergistic catalysis [the Fenton chemistry (38)] (39, 40), and the radical

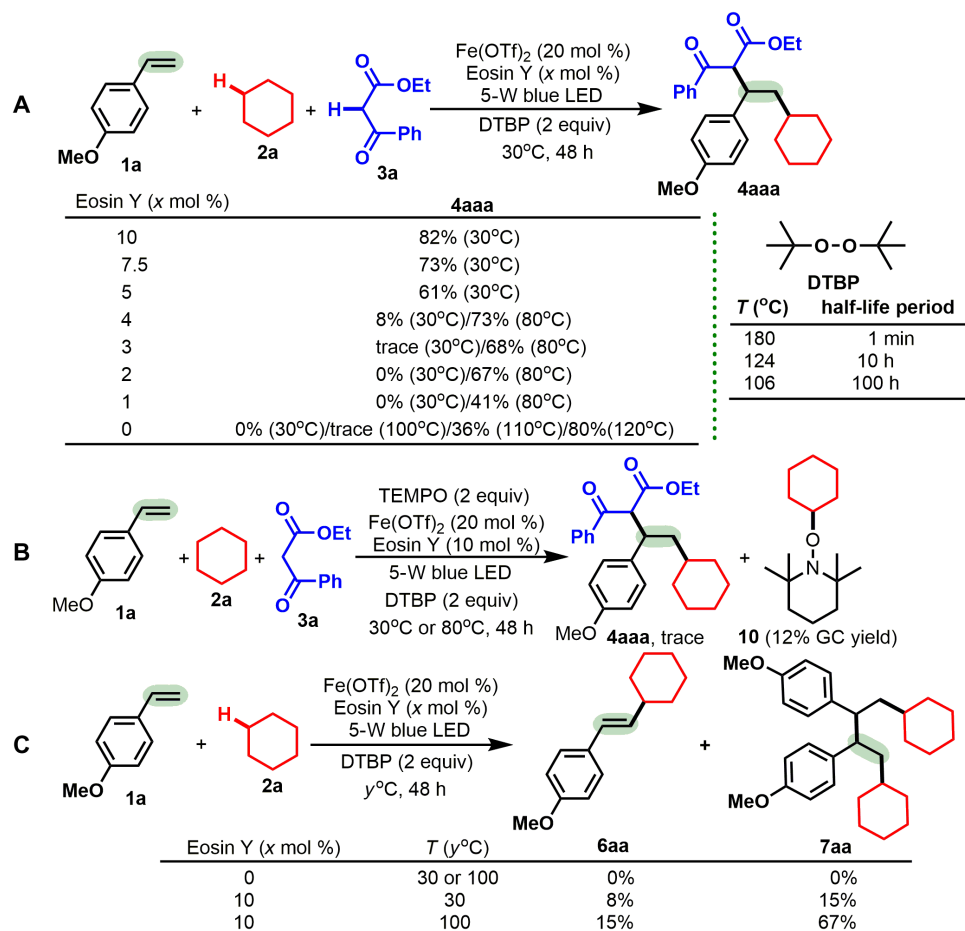


Fig. 2. Control experiments. (A) Loadings of Eosin Y on the reaction. (B) Trapping experiment with a stoichiometric amount of radical inhibitor. (C) Reaction between alkene **1a** and cyclohexane **2a** in the absence of dicarbonyl compounds.

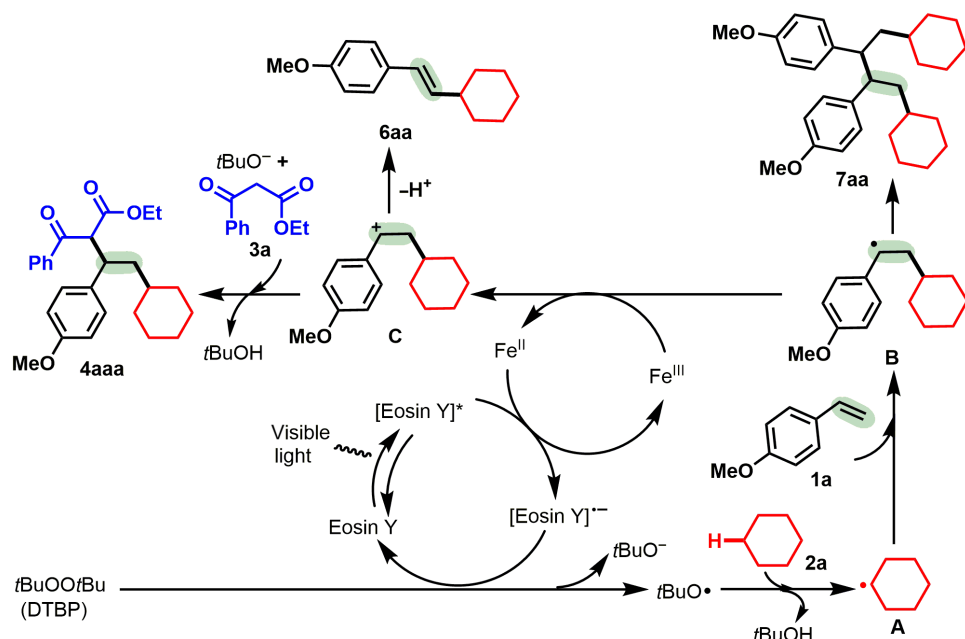


Fig. 3. Possible mechanism. The generation of cyclohexyl sp^3 -hybridized carbon-centered radical **A** and new alkyl radical intermediate **B** is supported by experimental evidence, and subsequent single-electron oxidation and nucleophilic reaction with 1,3-keto ester **3a** afford **4aaa**.

then abstracts a hydrogen from cyclohexane (**2a**) to afford sp^3 carbon-centered radical intermediate **A** (Fig. 3). Subsequently, addition of intermediate **A** across the C=C bond of alkene **1a** gives new alkyl radical intermediate **B**, which is supported by these results, including the formation of product **50a** from the reaction of alkene **1o** with cyclohexane **2a** (Table 2) (24) and two other by-products **6aa** and **7aa** from the reaction of alkene **1a** with cyclohexane **2a** at 60°C in the presence of methyl 3-oxobutanoate (Table 3 and Fig. 2C). Last, intermediate **B** undergoes single-electron oxidation via the cooperative effects of the active Fe(III) species (19–28), which is generated from the oxidation of the Fe(II) species by the [Eosin Y]* intermediate (29–37) to deliver carbocation intermediate **C** followed by nucleophilic reaction with 1,3-keto ester **3a** to access **4aaa**. Among these processes, the photoredox catalysis might assist in the single-electron oxidation step by regulating the oxidation and reduction potentials of the iron intermediates and the reaction partners (29–40).

In summary, we have established the first intermolecular unsymmetrical 1,2-dialkylation of alkenes with two distinct C(sp^3)–H bonds through cooperative photoredox and iron catalysis. The reaction allows concomitant incorporation of two vicinal alkyl groups across the C=C bond via dual C(sp^3)–H functionalization under mild conditions, and the method features high atom economy, excellent functional group tolerance, and broad substrate scopes with respect to both the sp^3 carbon-centered radical precursors (such as cycloalkanes, linear alkanes, and 1,4-dioxane) and the 1,3-dicarbonyl nucleophiles. This alkene dicarbofunctionalization reaction represents a novel and powerful strategy for the controlled functionalization of two or more different C(sp^3)–H bonds across an alkene or alkyne in a single reaction to access complex functionalized molecules through regulating the oxidation and reduction potentials of the iron intermediates and the reaction partners. Further studies on the applications of this new strategy for transforming petroleum-based feedstocks are currently underway.

MATERIALS AND METHODS

General procedure for intermolecular dialkylation of alkenes with two distinct C(sp^3)–H bonds enabled by synergistic photoredox catalysis and iron catalysis

Alkene **1** (0.2 mmol), alkane **2** (2 ml), 1,3-dicarbonyl **3** (0.3 mmol), Fe(OTf)₂ (20 mol %; 0.02 mmol), Eosin Y (10 mol %; 0.02 mmol), and DTBP (2 equiv; 0.4 mmol) were added to a Schlenk tube. Then the tube was charged with argon, and the mixture was stirred at the indicated reaction temperature (30° to 130°C) for 48 hours until complete consumption of starting material, as monitored by thin-layer chromatography and/or GC–mass spectrometry (MS) analysis. After cooling to room temperature, the mixture was filtered through a small plug of silica gel to remove the precipitate, and the plug was washed with EtOAc (3 × 10 ml). The solvent was then removed in vacuo, and the residue was further purified by silica gel flash column chromatography (10 to 40% ethyl acetate in hexane) to afford the desired product **4**.

SUPPLEMENTARY MATERIALS

Supplementary material for this article is available at <http://advances.sciencemag.org/cgi/content/full/5/3/eaav9839/DC1>

Section S1. General information and procedures

Section S2. Preliminary synthetic utilization

Section S3. Control experiments and mechanistic studies

Section S4. Analytical data for **4aaa** to **4naa**, **4paa** to **4qaa**, **4aba** to **4aha**, **4aab** to **4aan**, **50a**, **6aa**, **7aa**, **8aaa**, and **9aaa**

Fig. S1. Preliminary synthetic utilization.

Fig. S2. Control experiments.

Fig. S3. Profile of **4aaa** with the light on or off over time.

Fig. S4. Possible mechanisms.

Fig. S5. Cyclic voltammogram curves.

Fig. S6. Cyclic voltammogram curves.

Fig. S7. Cyclic voltammogram curves.

Fig. S8. Stern-Volmer fluorescence quenching experiments.

Fig. S9. ¹H, ¹³C-NMR spectra of product **4aaa**.

Fig. S10. ¹H, ¹³C-NMR spectra of product **4baa**.

Fig. S11. ¹H, ¹³C-NMR spectra of product **4caa**.

Fig. S12. ¹H, ¹³C-NMR spectra of product **4daa**.

Fig. S13. ¹H, ¹³C-NMR spectra of product **4eaa**.

Fig. S14. ¹H, ¹³C-NMR spectra of product **4faa**.

Fig. S15. ¹H, ¹³C-NMR spectra of product **4gaa**.

Fig. S16. ¹H, ¹³C-NMR spectra of product **4haa**.

Fig. S17. ¹H, ¹³C-NMR spectra of product **4iaa**.

Fig. S18. ¹H, ¹³C-NMR spectra of product **4jaa**.

Fig. S19. ¹H, ¹³C-NMR spectra of product **4kaa**.

Fig. S20. ¹H, ¹³C-NMR spectra of product **4laa**.

Fig. S21. ¹H, ¹³C-NMR spectra of product **4maa**.

Fig. S22. ¹H, ¹³C-NMR spectra of product **4naa**.

Fig. S23. ¹H, ¹³C-NMR spectra of product **4oaa**.

Fig. S24. ¹H, ¹³C-NMR spectra of product **3paa**.

Fig. S25. ¹H, ¹³C-NMR spectra of product **4aba**.

Fig. S26. ¹H, ¹³C-NMR spectra of product **4aca**.

Fig. S27. ¹H, ¹³C-NMR spectra of product **4ada**.

Fig. S28. ¹H, ¹³C-NMR spectra of product **4aea**.

Fig. S29. ¹H, ¹³C-NMR spectra of product **4afa**.

Fig. S30. ¹H, ¹³C-NMR spectra of product **4aga**.

Fig. S31. ¹H, ¹³C-NMR spectra of product **4aha**.

Fig. S32. ¹H, ¹³C-NMR spectra of product **4aab**.

Fig. S33. ¹H, ¹³C-NMR spectra of product **4aac**.

Fig. S34. ¹H, ¹³C-NMR spectra of product **4aad**.

Fig. S35. ¹H, ¹³C-NMR spectra of product **4aae**.

Fig. S36. ¹H, ¹³C-NMR spectra of product **4aaf**.

Fig. S37. ¹H, ¹³C-NMR spectra of product **4aag**.

Fig. S38. ¹H, ¹³C-NMR spectra of product **4aah**.

Fig. S39. ¹H, ¹³C-NMR spectra of product **4aai**.

Fig. S40. ¹H, ¹³C-NMR spectra of product **4aaj**.

Fig. S41. ¹H, ¹³C-NMR spectra of product **4aak**.

Fig. S42. ¹H, ¹³C-NMR spectra of product **4aal**.

Fig. S43. ¹H, ¹³C-NMR spectra of product **4aan**.

Fig. S44. ¹H, ¹³C-NMR spectra of product **50a**.

Fig. S45. (E)-1-(2-cyclohexylvinyl)-4-methoxybenzene (**6aa**).

Fig. S46. 4,4'-(1,4-Dicyclohexylbutane-2,3-diyl)bis(methoxybenzene) (**7aa**).

Fig. S47. ¹H, ¹³C-NMR spectra of product **8aaa**.

Fig. S48. ¹H, ¹³C-NMR spectra of product **8aaa**.

REFERENCES AND NOTES

- R. I. McDonald, G. Liu, S. S. Stahl, Palladium(II)-catalyzed alkene functionalization via nucleopalladation: Stereochemical pathways and enantioselective catalytic applications. *Chem. Rev.* **111**, 2981–3019 (2011).
- E. Merino, C. Nevado, Addition of CF₃ across unsaturated moieties: A powerful functionalization tool. *Chem. Soc. Rev.* **43**, 6598–6608 (2014).
- S. Tang, K. Liu, C. Liu, A. Lei, Olefinic C–H functionalization through radical alkenylation. *Chem. Soc. Rev.* **44**, 1070–1082 (2015).
- R. K. Dhungana, S. K. C. P. Basnet, R. Giri, Transition metal-catalyzed dicarbofunctionalization of unactivated olefins. *Chem. Rec.* **18**, 1314–1340 (2018).
- P. Basnet, S. K. C. P. Basnet, B. Shrestha, T. J. Boyle, R. Giri, Synergistic bimetallic Ni/Ag and Ni/Cu catalysis for regioselective γ,δ -diarylation of alkenyl ketimines: Addressing β -H elimination by in situ generation of cationic Ni(II) Catalysts. *J. Am. Chem. Soc.* **140**, 15586–15590 (2018).
- B. Shrestha, P. Basnet, R. K. Dhungana, S. K. C. P. Basnet, S. Thapa, J. M. Sears, R. Giri, Ni-catalyzed regioselective 1,2-dicarbofunctionalization of olefins by intercepting heck intermediates as imine-stabilized transient metallacycles. *J. Am. Chem. Soc.* **139**, 10653–10656 (2017).
- P. Basnet, R. K. Dhungana, S. Thapa, B. Shrestha, S. K. C. P. Basnet, J. M. Sears, R. Giri, Ni-catalyzed regioselective β,δ -diarylation of unactivated olefins in ketimines via ligand-enabled contraction of transient nickellacycles: Rapid access to remotely diarylated ketones. *J. Am. Chem. Soc.* **140**, 7782–7786 (2018).

- M. S. McCamant, L. Liao, M. S. Sigman, Palladium-catalyzed 1,4-difunctionalization of butadiene to form skipped polyenes. *J. Am. Chem. Soc.* **135**, 4167–4170 (2013).
- H. Cong, G. C. Fu, Catalytic enantioselective cyclization/cross-coupling with alkyl electrophiles. *J. Am. Chem. Soc.* **136**, 3788–3791 (2014).
- W. You, M. K. Brown, Diarylation of alkenes by a Cu-catalyzed migratory insertion/cross-coupling cascade. *J. Am. Chem. Soc.* **136**, 14730–14733 (2014).
- S. Thapa, P. Basnet, R. Giri, Copper-catalyzed dicarbofunctionalization of unactivated olefins by tandem cyclization/cross-coupling. *J. Am. Chem. Soc.* **139**, 5700–5703 (2017).
- A. Garcia-Dominguez, Z. Li, C. Nevado, Nickel-catalyzed reductive dicarbofunctionalization of alkenes. *J. Am. Chem. Soc.* **139**, 6835–6838 (2017).
- J. Derosa, V. T. Tran, M. N. Boulous, J. S. Chen, K. M. Engle, Nickel-catalyzed β,γ -Dicarbofunctionalization of alkenyl carbonyl compounds via conjunctive cross-coupling. *J. Am. Chem. Soc.* **139**, 10657–10660 (2017).
- S. KC, R. K. Dhungana, B. Shrestha, S. Thapa, N. Khanal, P. Basnet, R. W. Lebrun, R. Giri, Ni-catalyzed regioselective alkylation of vinylarenes via $C(sp^3)$ – $C(sp^3)$ / $C(sp^3)$ – $C(sp^2)$ bond formation and mechanistic studies. *J. Am. Chem. Soc.* **140**, 9801–9805 (2018).
- Z. Wu, D. Wang, Y. Liu, L. Huan, C. Zhu, Chemo- and regioselective distal heteroaryl ipso-migration: A general protocol for heteroarylation of unactivated alkenes. *J. Am. Chem. Soc.* **139**, 1388–1391 (2017).
- S. Thapa, R. K. Dhungana, R. T. Magar, B. Shrestha, S. KC, R. Giri, Ni-catalyzed regioselective 1,2-diarylation of unactivated olefins by stabilizing Heck intermediates as pyridylsilyl-coordinated transient metallacycles. *Chem. Sci.* **9**, 904–909 (2017).
- R. Giri, S. KC, Strategies toward dicarbofunctionalization of unactivated olefins by combined Heck carbometalation and cross-coupling. *J. Org. Chem.* **83**, 3013–3022 (2018).
- Z. Liu, T. Zeng, K. S. Yang, K. M. Engle, β,γ -Vicinal dicarbofunctionalization of alkenyl carbonyl compounds via directed nucleopalladation. *J. Am. Chem. Soc.* **138**, 15122–15125 (2016).
- A. J. McCarroll, J. C. Walton, Programming organic molecules: Design and management of organic syntheses through free-radical cascade processes. *Angew. Chem. Int. Ed.* **40**, 2224–2248 (2001).
- Z.-M. Chen, X.-M. Zhang, Y.-Q. Tu, Radical aryl migration reactions and synthetic applications. *Chem. Soc. Rev.* **44**, 5220–5245 (2015).
- H. Yi, G. Zhang, H. Wang, Z. Huang, J. Wang, A. K. Singh, A. Lei, Recent advances in radical C–H activation/radical cross-coupling. *Chem. Rev.* **117**, 9016–9085 (2017).
- W.-T. Wei, M.-B. Zhou, J.-H. Fan, W. Liu, R.-J. Song, Y. Liu, M. Hu, P. Xie, J.-H. Li, Synthesis of oxindoles by iron-catalyzed oxidative 1,2-alkylarylation of activated alkenes with an aryl $C(sp^3)$ –H bond and a $C(sp^3)$ –H bond adjacent to a heteroatom. *Angew. Chem. Int. Ed.* **52**, 3638–3641 (2013).
- J.-H. Fan, W.-T. Wei, M.-B. Zhou, R.-J. Song, J.-H. Li, Palladium-catalyzed oxidative difunctionalization of alkenes with α -carbonyl alkyl bromides initiated through a Heck-type insertion: A route to indolin-2-ones. *Angew. Chem. Int. Ed.* **53**, 6650–6654 (2014).
- A. Bunescu, Q. Wang, J. Zhu, Copper-catalyzed cyanomethylation of allylic alcohols with concomitant 1,2-aryl migration: Efficient synthesis of functionalized ketones containing an α -quaternary center. *Angew. Chem. Int. Ed.* **54**, 3132–3135 (2015).
- X.-H. Ouyang, R.-J. Song, M. Hu, Y. Yang, J.-H. Li, Silver-mediated intermolecular 1,2-alkylarylation of styrenes with α -carbonyl Alkyl bromides and indoles. *Angew. Chem. Int. Ed.* **55**, 3187–3191 (2016).
- Z. Li, Y. Zhang, L. Zhang, Z.-Q. Liu, Free-radical cascade alkylation of alkenes with simple alkanes: Highly efficient access to oxindoles via selective (sp^3) C–H and (sp^2) C–H bond functionalization. *Org. Lett.* **16**, 382–385 (2014).
- H. Wang, L.-N. Guo, X.-H. Duan, Silver-catalyzed decarboxylative acylation of acrylamides with α -oxocarboxylic acids in aqueous media. *Adv. Synth. Catal.* **355**, 2222–2226 (2013).
- M.-B. Zhou, R.-J. Song, X.-H. Ouyang, Y. Liu, W.-T. Wei, G.-B. Deng, J.-H. Li, Metal-free oxidative tandem coupling of activated alkenes with carbonyl $C(sp^3)$ –H bonds and aryl $C(sp^3)$ –H bonds using TBHP. *Chem. Sci.* **4**, 2690–2694 (2013).
- C. K. Prier, D. A. Rankic, D. W. C. MacMillan, Visible light photoredox catalysis with transition metal complexes: Applications in organic synthesis. *Chem. Rev.* **113**, 5322–5363 (2013).
- M. N. Hopkinson, B. Sahoo, J.-L. Li, F. Glorius, Dual catalysis sees the light: Combining photoredox with organo-, acid, and transition-metal catalysis. *Chem. Eur. J.* **20**, 3874–3886 (2014).
- J.-R. Chen, X.-Q. Hu, L.-Q. Lu, W.-J. Xiao, Visible light photoredox-controlled reactions of *N*-radicals and radical ions. *Chem. Soc. Rev.* **45**, 2044–2056 (2016).
- J.-R. Chen, X.-Q. Hu, L.-Q. Lu, W.-J. Xiao, Exploration of visible-light photocatalysis in heterocycle synthesis and functionalization: Reaction design and beyond. *Acc. Chem. Res.* **49**, 1911–1923 (2016).
- L. Shi, W. Xia, Photoredox functionalization of C–H bonds adjacent to a nitrogen atom. *Chem. Soc. Rev.* **41**, 7687–7697 (2012).
- X.-Q. Hu, J.-R. Chen, W.-J. Xiao, Controllable remote C–H bond functionalization by visible-light photocatalysis. *Angew. Chem. Int. Ed.* **56**, 1960–1962 (2017).
- J. Zhang, Y. Li, F. Zhang, C. Hu, Y. Chen, Generation of alkoxy radicals by photoredox catalysis enables selective $C(sp^3)$ –H functionalization under mild reaction conditions. *Angew. Chem. Int. Ed.* **55**, 1872–1875 (2016).
- G. J. Choi, Q. Zhu, D. C. Miller, C. J. Gu, R. R. Knowles, Catalytic alkylation of remote C–H bonds enabled by proton-coupled electron transfer. *Nature* **539**, 268–271 (2016).
- J. C. K. Chu, T. Rovis, Amide-directed photoredox-catalysed C–C bond formation at unactivated sp^3 C–H bonds. *Nature* **539**, 272–275 (2016).
- C. Walling, Fenton's reagent revisited. *Acc. Chem. Res.* **8**, 125–131 (2002).
- S. Zou, Y. Shi, Organic peroxide TBPV & DTBP and their applications. *Petrochem. Ind. Trends* **5**, 39 (1997).
- E. T. Denisov, T. G. Denisova, T. S. Pokidova, *Handbook of Free Radical Initiators* (John Wiley & Sons Inc., 2003), chap. 4, pp. 61–97.

Acknowledgments

Funding: We thank the National Natural Science Foundation of China (nos. 21625203 and 21472039), the Jiangxi Province Science and Technology Project (nos. 20171ACB20015 and 20165BCB18007), and the Opening Fund of Key Laboratory of Chemical Biology and Traditional Chinese Medicine Research (Hunan Normal University), Ministry of Education (no. KLCBTCMR18-02) for financial support. **Author contributions:** X.-H.O., Y.L., R.-J.S., M.H., S.L., and J.-H.L. conceived the project, wrote the manuscript, and analyzed the data. X.-H.O., Y.L., R.-J.S., and M.H. performed the experiments. **Competing interests:** The authors declare that they have no competing interests. **Data and materials availability:** All data needed to evaluate the conclusions in the paper are present in the paper and/or the Supplementary Materials. Additional data related to this paper may be requested from the authors.

Submitted 9 November 2018

Accepted 6 February 2019

Published 29 March 2019

10.1126/sciadv.aav9839

Citation: X.-H. Ouyang, Y. Li, R.-J. Song, M. Hu, S. Luo, J.-H. Li, Intermolecular dialkylation of alkenes with two distinct $C(sp^3)$ –H bonds enabled by synergistic photoredox catalysis and iron catalysis. *Sci. Adv.* **5**, eaav9839 (2019).